Journal of Electroanalytical Chemistry 967 (2024) 118491

Contents lists available at ScienceDirect

Journal of Electroanalytical Chemistry

journal homepage: www.elsevier.com/locate/jelechem

Electroless plating of Co—P—O electrocatalyst on carbon cloth for alkaline water electrolysis

Pooja J. Sharma [a], Sohel Siraj [b], Parikshit Sahatiya [b], C.K. Sumesh [a], Pratik M. Pataniya [a,*]

[a] Department of Physical Science, P. D. Patel Institute of Applied Sciences, Charotar University of Science and Technology, CHARUSAT, Changa 388421, Gujarat, India
[b] Department of Electrical and Electronics Engineering, Birla Institute of Technology and Science Pilani Hyderabad Campus, Hyderabad 500078, India

ARTICLE INFO

Keywords:
Electroless plating
Co–P–O nanoparticles
Fabric electrodes
Electrolysis
Hydrogen energy

ABSTRACT

We report the simple method of fabrication, self-supported nanostructure of Co—P—O nanoparticles (NPs) on carbon cloth scaffold by electroless plating. Co—P—O demonstrates exceptional bi-functional catalytic performance in water electrolysis, efficiently producing hydrogen (H_2) and oxygen (O_2) gases simultaneously due to optimized adsorption energy for intermediates and the excellent conductivity of Cobalt-metallic nanoparticles. Co—P—O achieves a geometric current of 10 mA/cm^2 with 190 mV and 280 mV overpotential for hydrogen evolution reaction (HER) and oxygen evolution reaction (OER), respectively, while its continuous catalytic nanoparticle coating on the carbon cloth scaffold ensures superior charge transport with minimal resistance. It is highly encouraging to observe that the HER and OER performance of Co—P—O electrodes far surpasses that of carbon cloth, approaching the benchmark set by noble electrocatalysts Pt/C and RuO_2. The alkaline electrolyser based on the two-electrode cell using Co—P—O electrodes demonstrates bi-functional water splitting at 1.64 V and 1.98 V at 10 and 100 mA/cm^2. Furthermore, the alkaline electrolyser exhibits stable electrocatalytic activity for about more than 16 h at the current density of 50 mA/cm^2.

1. Introduction

Designing affordable, sustainable, and highly efficient energy alternatives to decrease the dependence on fossil fuels is extremely desirable in view of the world's energy crisis and major environmental pollution problems [1–4]. One of the most potential next-generation renewable green energy sources, molecular hydrogen (H_2) has high gravimetric energy value (150 MJ/kg) and ecologically acceptable nature [5–10]. Among various techniques to produce hydrogen, splitting water into its constituents is a promising and sustainable technique. The water electrolysis facilitates two half-reactions one is the hydrogen evolution reaction (HER) and the second is the oxygen evolution reaction (OER) [11–13]. The tendency of intermediate *H to adsorb on catalyst surfaces is a key factor in the HER process. In addition, the OER reaction is sluggish because creating a reaction intermediate *O or forming a reaction intermediate *OOH hinders the OER process. Thus, the creation of bi-functional catalysts which can speed up the HER and OER, and improve sustainable hydrogen production are essential [14–17].

Among various earth-abundant, bifunctional electrocatalysts, cobalt in conjunction with chalcogenides/oxide/hydroxide has shown great promise for catalytic water electrolysis because of their low cost, and small energy barrier for H adsorption etc [18–22]. It has been noted that metal phosphides exhibit strong electrical conductivity, which could be attributed to the presence of metal–metal bonding inside the phosphides and rich active sites. Phosphorus in CoP helps to control the electron density of Co sites, which improves the capacity for hydrogen adsorption and electron transport while decreasing hydrogen adsorption to increase the activity of the HER. Additionally, the oxidation structure of phosphorus is more beneficial to the corresponding OER. Furthermore, phosphorus has the potential to lower the free energy in the HER process, which is better for boosting the stability of the OER and HER catalytic processes [23,24].

The electrode's design (electrocatalyst plus current collector, unique morphology e.g. NWs, NSs, hollow structures, NPs, etc.) is another essential component that influences the overall water-splitting process [25]. We need to prepare the large area and polymeric binder-free catalysts. In order to build durable and effective catalytic electrodes, substrate materials are essential. Due to their high conductivity and ease of loading, many metals such as titanium, iron, and nickel, in the form of foil or foam are currently the most common substrate materials for electrodes. Although these substrates offer good mechanical and electrical conductivity, they also have certain inherent drawbacks, such as

* Corresponding author.
E-mail address: pm.pataniya9991@gmail.com (P.M. Pataniya).

https://doi.org/10.1016/j.jelechem.2024.118491
Received 25 April 2024; Received in revised form 26 June 2024; Accepted 4 July 2024
Available online 6 July 2024

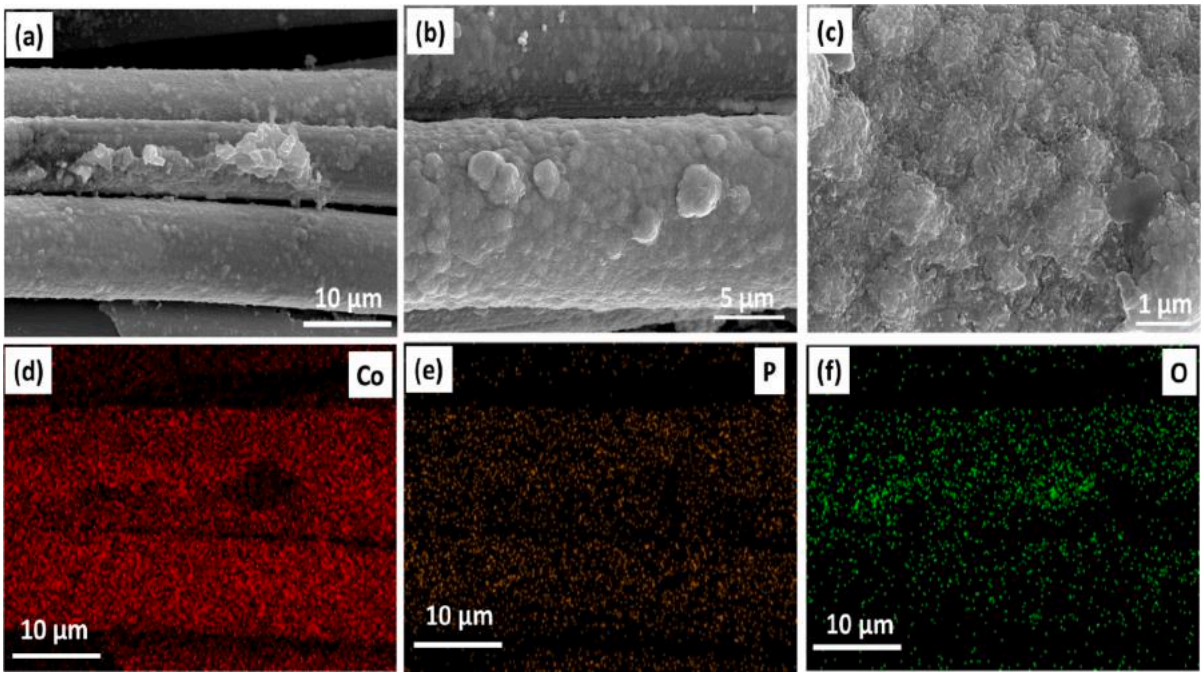

Fig. 1. (a–c) SEM image of the fabric electrode, (d–f) SEM-EDS elemental mapping of Co, P, and O on the Co—P—O fabric electrode.

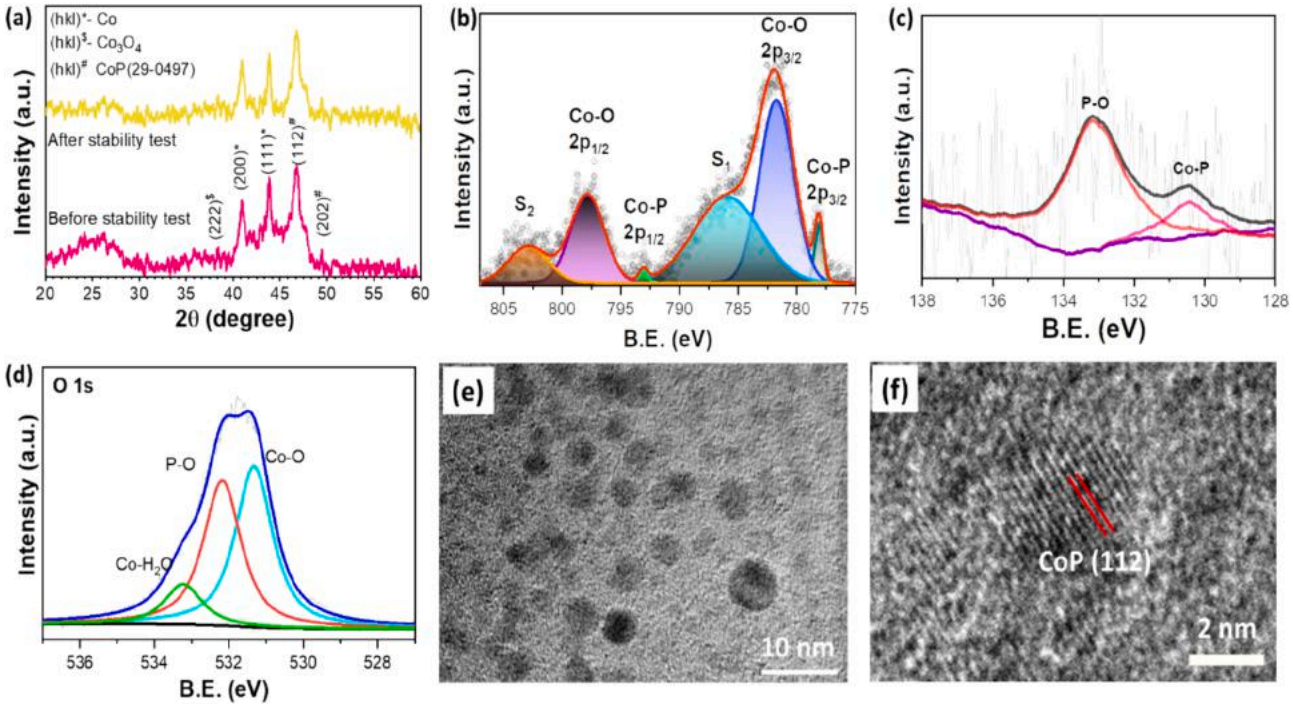

Fig. 2. (a) Powder XRD pattern of Co—P—O fabric, XPS spectrum of elements of CoP fabric (b) Co 2p, (c) P 2p, (d) O 1s and (e and f) HRTEM images of CoP.

high cost, limited flexibility, heaviness, and environmental problems [26–28]. Carbon cloth offers inherent advantages as an electrode substrate material such as excellent electrical conductivity which allows carbon cloth to be easily coupled to surface catalysts, lowering the electron conduction resistance during the catalytic process, and staggered porous structure facilitates reactant transport and speeds up bubble escape [29].

Based on that, Lvlv Ji and their group developed CoP NFs by precipitation, chemical etching and low-temperature phosphidation process for overall water splitting. They reported that CoP nano-frame electrocatalyst required only 1.65V to reach at 10mA/cm^2 current density [30]. CoP NPs embedded *N*-doped carbon nanotube hollow polyhedrons were demonstrated by Pan et al., exhibiting prominent attributes such as high surface area and well-defined inner channels. These features are highly advantageous in promoting efficient charge and mass transport during electrocatalysis [31]. In order to change the surface structure and increase the density of O_h Co^{3+} in OER, Han et al. introduced Zn into the Co_3O_4 lattice. This boosted the electrocatalytic ability [1]. Highly conductive and flexible carbon cloth (CC) gives us new 3D support to incorporate HER, OER, and OWS catalysts for use in

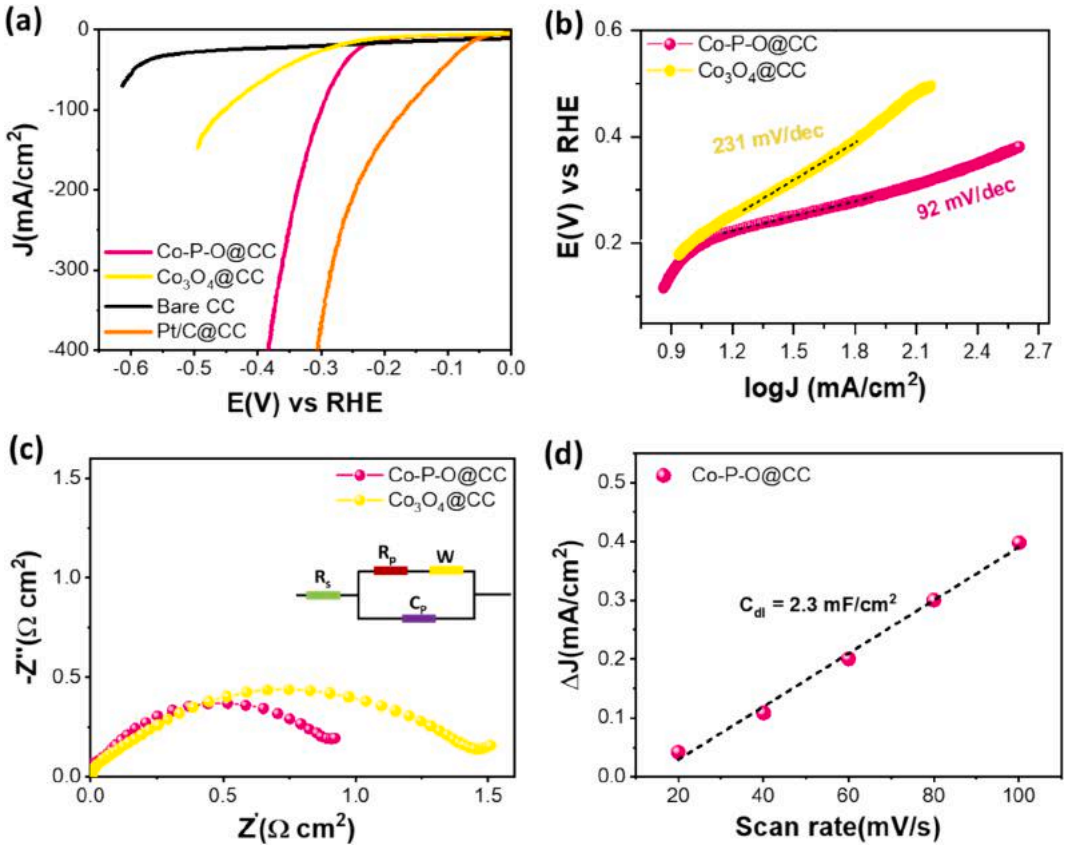

Fig. 3. (a) Polarization curves for HER performance on Co—P—O fabric, Co_3O_4@CC, carbon cloth (CC) and commercial Pt/C@CC in 1.0 M KOH with iR compensation, (b) Tafel plots obtained from polarization curves, (c) EIS plot, (d) ΔJ vs scan rate for calculation double layer capacitance (C_{dl}).

technological gadgets [19]. Additionally, porous nanoparticles of cobalt sulphide (CoS) have demonstrated efficient electrocatalytic HER in acidic and alkaline medium owing to fast charge transfer and higher electrochemical surface area [32].

Electroless plating-coated metal electrodes have shown significant promise for water-splitting applications owing to their efficient catalytic performance, stability, and low-cost [14,33]. The electroless plating method is a facile process that enables the uniform deposition of a thin layer of a catalytically active metal onto the surface of electrodes, thus enhancing their catalytic performance. In addition, this process has also been carried out in less time and the equipment for manufacturing electroless plating deposition is not complex [34,35]. The electroless plating process is also employed for the deposition of catalysts on a non-conducting substrate and converting it to highly conducting electrode which showed uniform metal layer over a large scale. Such properties are useful for various energy conversion and storage applications. Typically, the electroless plating deposition involves the metal ions reduction in solution using a strong reducing agent, which helps to control the deposition rate and the morphology of the deposited metal layer [36]. The deposited metal layer facilitates catalytic sites for the HER and OER during water electrolysis [37]. In electroless deposition, ionic ions are reduced through the reducing agent (hypophosphite, and catalysts (Pd^0). Initially, the carbon cloth is sensitized by the Sn^{+2} and then activated by the Pd^{+2} (Eq. (1)). Secondly, the Pd^0 catalyzes the reduction of Co^{+2} in the presence of NaH_2PO_2 (Eq. (2)). A secondary reaction between hypophosphite and atomic hydrogen results in the formation of phosphorous ($H_2PO_2^- + H \rightarrow P + OH^- + H_2O$) [14,38–40].

$$Pd^{+2} + Sn^{+2} \rightarrow Sn^{+4} + Pd^0 \quad (1)$$

$$Co^{+2} + H_2PO_2^- + H_2O \rightarrow Co + H_2PO_3^- + 2H^+ \quad (2)$$

Inspired from this, we demonstrate the electroless deposition of Co—P—O electrocatalysts on carbon cloth. As prepared Co—P—O shows efficient HER and OER performance with high current density of 400 mA/cm^2, approaching the noble catalysts Pt/C and RuO_2-like performance. Self-supported catalytic network shows the bi-functional electrolysis with geometric current of 100 mA/cm^2 at 1.98 V owing to the nanostructured structure and high intrinsic activity.

2. Experimental section

2.1. Chemicals and reagents

Tin chloride dihydrate ($SnCl_2{\cdot}2H_2O$), palladium(ll) chloride ($PdCl_2$) (99.0 %, HIMedia Pvt. Ltd., INDIA), cobalt sulfate heptahydrate ($CoSO_4{\cdot}7H_2O$), tri-sodium citrate ($Na_3C_6H_5O_7$), sodium hypophosphite monohydrate ($NaH_2PO_2{\cdot}H_2O$), were purchased from Merck Pvt. Ltd., India. Ammonia chloride (NH_4Cl), potassium hydroxide powder (KOH), hydrochloric acid (HCl), and carbon-cloth were purchased from Techinstro, India. All of the reagents were analytic purity grade and were employed directly.

2.2. Preparation of Co—P—O fabric electrodes

The carbon-cloth (CC) were used as a substrate for the deposition of cobalt nanoparticles by electroless plating process. The CC pieces were cleaned in 2.5 M HCl and distilled water to eliminate the impurities. Firstly, a cleaned CC of dimensions 5 × 5 cm was immersed in a solution containing 1.2 g tin chloride dihydrate ($SnCl_2{\cdot}2H_2O$), and 0.24 M of hydrochloric acid (HCl) in 50 ml water for sensitization for 30 min. Then, the CC was nicely cleaned with water and acetone after sensitization and dried in a vacuum oven at 70 °C for 20 min. Subsequently, the

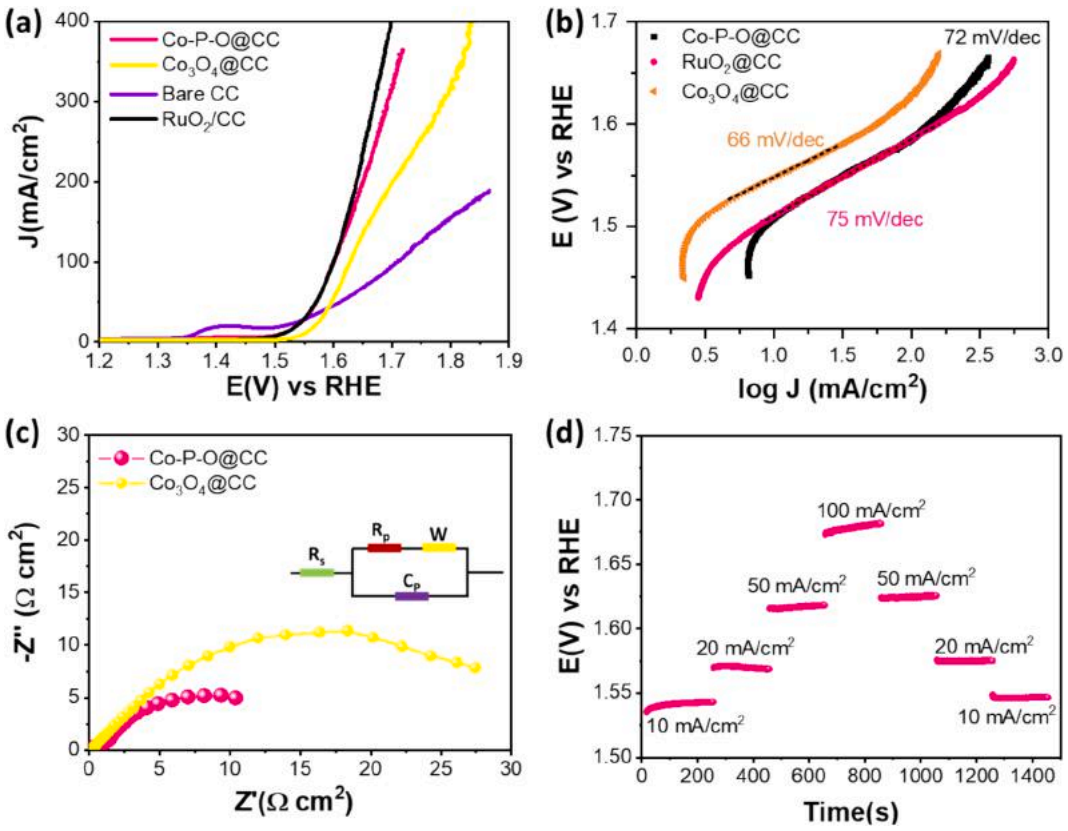

Fig. 4. (a) Polarization curves for OER performance on Co—P—O fabric, Co_3O_4@CC, carbon cloth (CC) and commercial RuO_2C@CC in 1.0 M KOH with iR compensation, (b) Tafel plots obtained from polarization curves, (c) EIS plot, (d) Step chrono-potentiometry curves for Co—P—O fabric at different current density.

as-sensitized CC was dipped in 50 ml solution containing 0.012 g palladium (II) chloride ($PdCl_2$) and 0.24 M of HCl solution for activation. The activated CC was washed using water and acetone and dried at 70 °C. Finally, the activated carbon cloth with decorated Pd nanoparticles was transferred in our lab-made electroless plating bath maintained at 60 °CC containing 1.125 g cobalt sulfate heptahydrate ($CoSO_4{\cdot}7H_2O$), 2.064 g trisodium citrate ($Na_3C_6H_5O_7$), 1.694 g sodium hypophosphite monohydrate ($NaH_2PO_4{\cdot}H_2O$), and 8 ml ammonia solution for 45 min for deposition of Co—P—O nanoparticles. The carbon cloth was properly cleaned with acetone and DI water after electroless plating, and then it was dried for overnight at 80 °C.

2.3. Material characterizations

Firstly, the structure of the Co—P—O catalyst was characterized by powder XRD using D2 phaser BRUKER, λCu Kα = 0.15418 nm. The morphology, chemical purity, and elemental mapping of Co—P—O NPs carbon cloth (CC) was investigated by using FE-SEM/EDS (Make: TESCAN and Bruker, MIRA 3(FESEM) and Quantax 200 (EDS), Evactron XEI (plasma cleaner)). The surface chemical composition and the electronic structure of the Co—P—O was investigated by X-ray photoelectron spectroscopy (XPS) (Make: SPECS Surface Nano Analysis GmbH, Germany). Furthermore, the morphology and structure was investigated by HR-TEM.

2.4. Electrochemical measurements

The electrocatalytic water electrolysis on Co—P—O based fabric electrodes was studied in alkaline electrolyte (1M KOH) using METROHM-PGSTAT/M204 workstation. The HER and OER performance of Co—P—O electrodes (area: 1 × 1 cm^2) was studied using standard three electrodes system having Co—P—O electrodes, graphite rod, and 3 M KCl saturated Ag/AgCl as working, counter, and reference electrode, respectively. The control electrodes such as Co_3O_4@CC and bare CC were also analysed in identical condition. Firstly, the electrochemical performance was studied by linear sweep voltammetry curves at scan rate of 2 mV/s. The overpotential were determined for HER and OER to generate the benchmark geometric current of 10 mA/cm^2. The potential was determined with respect to the standard reversible hydrogen electrode (RHE) using the following equation: $E_{RHE} = 0.1976 + E_{Ag/AgCl} + (0.059 \times pH)$. The Tafel plots were also calculated from the LSVs to study the kinetic of the HER and OER for all the electrodes. Further, cyclic-voltammetry curves were recorded for the calculation of double layer capacitance (C_{dl}) and electrochemically active surface area (ECSA = C_{dl}/C_e, where, C_e is the specific capacitance = 0.04 mF/cm^2 in alkaline electrolyte). The electrochemical impedance spectroscopy was used to study the charge-transport mechanism in the electrodes. By knowing the capabilities of Co—P—O electrodes for HER and OER, an alkaline electrolyser having Co—P—O electrodes as both anode and cathode was prepared to study the overall water splitting. LSV curves, multi-step chrono-potentiometry curves were recorded to study the overall water splitting and cell voltage required to generate the benchmark current density 10 and 100 mA/cm^2 were determined. The stability of the Co—P—O electrodes for overall water splitting was measured at 50 mA/cm^2 for 16 h in 1M KOH.

3. Result and discussion

The Co—P—O electrocatalysts was deposited on the carbon cloth (CC) for fabrication of flexible and large-area electrodes for alkaline electrolysis of water. The morphology of the Co—P—O electrocatalyst on CC was investigated by SEM and EDS elemental mapping. As evident from Fig. 1-a, the abundant voids throughout the scaffold, the microstructure of carbon cloth is not affected by self-catalysed and closely

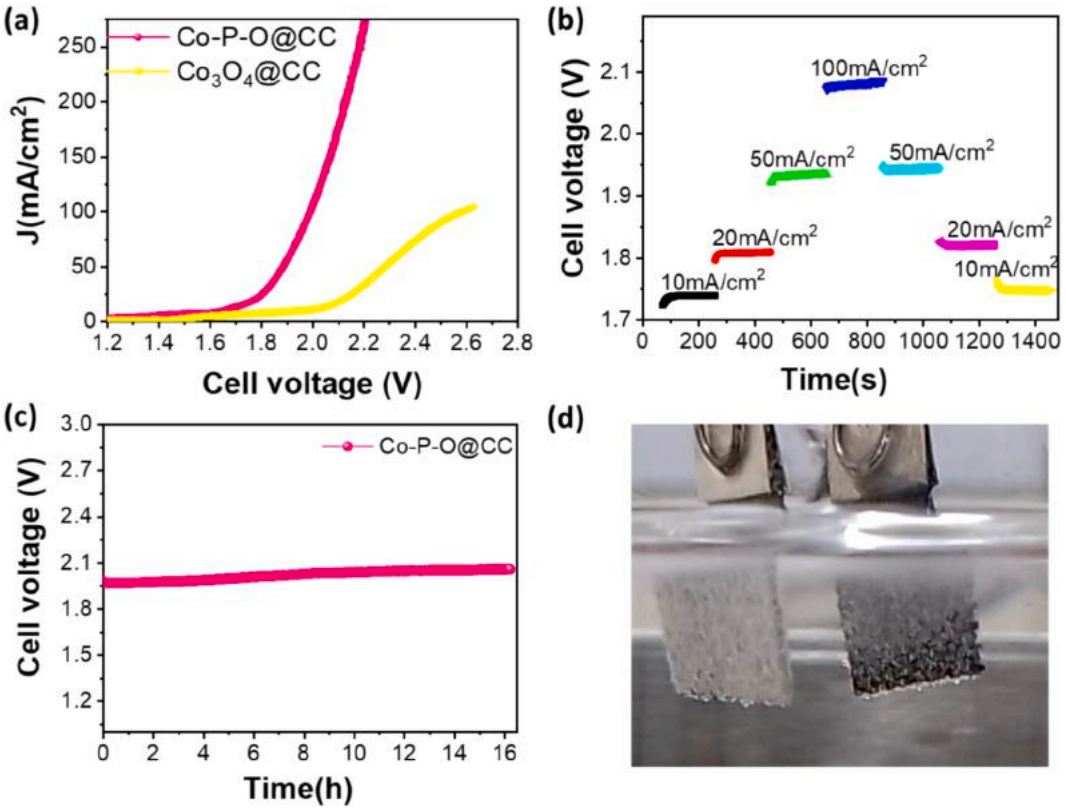

Fig. 5. (a) Polarization curve with iR compensation for overall water splitting using Co—P—O two electrode setup in 1 M KOH, (b) multi-step chrono-potentiometry without iR compensation, (c) Chrono-potentiometry for long-term stability measurement at 50 mA/cm^2 without iR compensation, (d) digital image of evolution of hydrogen and oxygen from Co—P—O electrodes.

packed Co—P—O NP coating. Fig. 1-a-c shows the uniformly anchored Co—P—O electrocatalyst NP on the fabric scaffold, which was further validated by EDS-mapping of the Co, P, and O-element (Fig. 1-d-f). The weight percentage of the Co, P, O and C measured by EDS are 84 %, 1 %, 4 % and 16 %, respectively (Fig. S1, Supporting information).

The structure of the Co—P—O fabric was studied by powder XRD, as shown in Fig. 2-a. XRD pattern shows the weak peaks corresponding to metallic CoP, Co and Co_3O_4 compositions [41,42]. The surface chemical composition and the electronic states of the Co—P—O—fabric were further studied by XPS analysis. Fig. 2-b shows the high-resolution XPS spectrum of Co 2p, which is de-convoluted into 6 peaks. The peaks centered at 778.08 eV and 793.06 eV are assigned to Co^{2+} $2p_{3/2}$ and Co^{2+} $2p_{1/2}$, confirms the presence of CoP phase [41,42]. Two peaks at binding energies of 781.72 eV (Co^{2+} $2p_{3/2}$) and 797.84 eV (Co^{2+} $2p_{1/2}$) shows the presence Co-O interaction, which confirms the presence of Co_3O_4 phase [41,42]. The other two peaks at binding energies 786.0 and 802.9 eV ate the satellite peaks of Co^{2+} which are observed due to exposure of Co-fabric in an ambient environment [43,44]. XPS spectrum of P 2p shows the peak centered at 130.45 eV and 133.21 eV shows the Co–P and P—O bond, respectively [43,44]. Fig. 1-d shows the XPS spectra of O1s, containing peaks centered at 531.35eV, 532.19 eV and 533.24 eV shows the Co-O, P—O, and Co-H_2O interactions [41,42]. The presence of Co-O offers a potential catalytic activity for effective oxygen evolution reaction. Fig. S3 shows the XPS spectra of Pd, showing the absence of Pd from the Co—P—O electrode. The structure of the catalytic nanoparticles extracted from the Co—P—O fabric was analyzed by HRTEM. The nanoparticles of dimensions less than 10 nm laterals dimension are seen in Fig. 2-e. At higher resolution, the Co–P nanoparticle having (1 1 2) orientation is detected (Fig. 2-f), confirms the presence of CoP phase in Co—P—O fabric. The Co_3O_4 phase was not detected in the HRTEM image due to amorphous nature, which is also supported by the powder XRD. Despite having low HER activity, Co_3O_4 is a very effective OER electrocatalyst. However, P may be successfully doped to greatly increase the catalyst's HER and OER activities [45]. The aforementioned characteristics unequivocally confirm to the successful fabrication of Co–P and the corresponding oxide (Co–O and P—O) catalytic electrode.

3.1. Hydrogen evolution reaction

The electrocatalytic HER performance of the as prepared Co—P—O fabric is studied in 1.0 M KOH aqueous solution using a standard three-electrode system. For the comparison, control electrodes like Co_3O_4@CC, commercial Pt/C@CC, and bare carbon cloth (CC) are also tested in identical condition. Fig. 3-a shows the polarization curve of the as prepared electrodes. As expected, Co_3O_4@CC and bare CC exhibit extremely inferior HER performance. Electroless deposited Co—P—O fabric demonstrates the obvious HER performance with an overpotential of $\eta = 190$ mV@10 mA/cm^2, and $\eta = 300$ mV@100 mA/cm^2. Although, this HER performance is inferior to noble Pt/C-based electrode, the Co—P—O fabric shows superior HER performance compared to previously reported state-of-the-art catalyst based on non-noble metals such as WSe_2 [46], NiS [47], CoS [32], ReS_2 [48], etc. in alkaline electrolysers. According to the literature, in the HER mechanism of CoP, the phosphorous sites function as proton-acceptor centres, and the cobalt sites as hydride-acceptors. The CoP catalyst facilitates the facile adsorption of protons to produce cobalt hydride species for subsequent hydrogen evolution.

The Tafel slope for Co—P—O is about 92 mV/dec (Fig. 3-b), suggesting that the HER on Co—P—O catalyst is accomplished by the Volmer-Heyrovsky mechanism in alkaline media [49,50]. To investigate the HER kinetics for Co—P—O fabric, electrochemical impedance spectroscopy (EIS) was used as shown in Fig. 3-c. The corresponding equivalent circuit of the fitted Nyquist plots is also displayed in the inset

Table 1
Comparison of the electrocatalytic HER, OER, and OWS activity between the Co-P_O@CC NPs and other recently reported catalysts.

Materials/ Electrode	Electrolytes/ Reaction	Overpotential $\eta_j = 10$ mA/ cm^2	Tafel Slope (mV/ dec^{-1})	Stability Time (h)	Ref.
Co—P—O@CC NPs	1.0 M KOH (HER)	205	92	–	This work
	1.0 M KOH (OER)	280	72	–	
	1.0 MKOH (OWS)	1.64 V	–	16	
NiFeP@FP	1.0 M KOH (HER)	158	–	–	[57]
	1.0 M KOH (OER)	282	82.36	–	
	1.0 MKOH (OWS)	1.62 V	–	30	
$Ni_{0.83}Co_{0.17}P$/NF	1.0 M KOH (OER)	295	45	25	[58]
NiCoP/C	1.0 M KOH (OER)	315	87	14	[59]
NiCoP-Se	1.0 M KOH (OER)	340	87	24	[60]
CoP/rGO	1.0 M KOH (HER)	154	–	10	[61]
	1.0 M KOH (OER)	292	80	10	
	1.0 MKOH (OWS)	1.63 V	–	–	
CoP nanowires/ carbon cloth	1.0 M KOH (OER)	209	129	–	[21]
CoP nanoneedles/ carbon cloth	1.0 M KOH (HER)	95	60	–	[62]
	1.0 M KOH (OER)	281	62	17	
	1.0 MKOH (OWS)	1.63 V	119	72	
Co–P nanospheres/ FTO	1.0 M KOH (HER)	125	54	10	[20]
	1.0 M KOH (OER)	420	83	10	
CoP mesoporous nanorod arrays	1.0 M KOH (HER)	54	51	–	[63]
	1.0 M KOH (OER)	310	65	–	
	1.0 MKOH (OWS)	1.62 V	–	32	
CoP/C	1.0 M KOH (OER)	330	53	25	[64]
CoP_2/RGO	1.0 M KOH (OER)	300	96	2.5 h	[65]
	1.0 MKOH (OWS)	1.65 V		2.5 h	
CoP/rGO	1.0 M KOH (HER)	150	38	22	[66]
	1.0 M KOH (OER)	340	66	22	
	1.0 MKOH (OWS)	1.7 V		–	
CoP/o-CC	1.0 M KOH (HER)	95.45 mV	96.4	–	[29]
$Ni_{0.6}Co_{1.4}P$	1.0 M KOH (OER)	300 mV	80	10	[67]
$NiCo_2O_4$/NiCoP	1.0 M KOH (HER)	198 mV	91	12	[68]
	1.0 M KOH (OER)	295 mV	70	12	
	1.0 MKOH (OWS)	1.66 V	–	12	

of Fig. 3-c. The R_s and R_{ct} represent the solution resistance and charge transfer resistance respectively. The EIS data reveal that Co—P—O exhibits a small value of charge transfer resistance (R_{ct} = 1.2 Ω•cm^2), compared to Co_3O_4 suggesting an accelerated Faradaic process and faster electron transfer [51–53]. Furthermore, the double-layer capacitance (C_{dl}) at the electrolyte–electrode interface was measured to calculate the electrochemically active surface areas (ECSA) using cyclic voltammetry at various scan rates from 10 to 100 mV/s within a non-Faradaic potential range (Fig. S4). The C_{dl} value of Co—P—O was estimated to be around 2.3 mF/cm^2 (Fig. 3-d). ECSA was also calculated using the following equation (ECSA = C_{dl}/C_e, where, C_e = 0.04 mF/cm^2, the capacitance of an atomically smooth planar surface in an alkaline medium). ECSA for Co—P—O electrodes is 57.5 cm^2. Fig. S5 illustrates a multi-step chrono-potentiometry curve generated at Co—P—O in 1.0M KOH at current density varying from 10 to 100 mA/cm^2 which demonstrates the rapid change in potential on switching the cathodic current due to effective and stable electronic and mass transport [54].

3.2. Oxygen evolution reaction

The OER performances of the Co—P—O were also investigated under alkaline conditions and compared with the Co_3O_4@CC, bare CC, and commercial RuO_2@CC. Fig. 4-a shows the polarization curves for the OER activity of electrodes, showing that Co—P—O requires a potential of 1.51 V (1.60 V) and an overpotential of 280 mV (370 mV) to generate geometric current density of 10 mA/cm^2 (100 mA/cm^2). The OER performance of Co—P—O is almost similar to commercial RuO_2/CC catalysts, showing that the Co—P—O electrodes is one of the efficient substitutes of noble-OER catalysts. This implies that Co—P—O exhibits optimized *OH intermediate adsorption and enable the simple desorption of oxygen molecules at the anode [2,9]. Fig. 4-b shows that Co—P—O exhibits small Tafel slope than Co_3O_4 due to the accelerated OER performance on Co—P—O catalysts. Tafel slope for Co—P—O catalyst showed the lowest value of 52 mV/dec, confirming the favourable OER kinetics on the Co—P—O surface. The enhanced activity of Co—P—O fabric is also attributed to the fast electronic accessibility which can be observed from the Nyquist plot as shown in Fig. 4-c. The Co—P—O exhibits low R_{ct} of around 15 Ω•cm^2 as compared to 38 Ω•cm^2 for Co_3O_4@CC, suggesting the higher conductivity and fast charge transport for Co—P—O electrode [55,56]. Multi-step chrono-potentiometry curve shows the excellent stability towards the OER performance and stable charge and mass transport, as shown in Fig. 4-d. With the switching of current from 10 to 100 mA/cm^2, the potential remains stable and changes sharply, demonstrating stable charge transport, mass transfer, and structural integrity of the Co—P—O fabric.

3.3. Overall water splitting

Encouragingly, the two-electrode alkaline electrolyser for bi-functional water splitting using Co—P—O fabric as anode and cathode was developed (Fig. 5-d). Fig. 5-a shows the polarization curve for electrolysis, showing the overall water splitting (OWS) and simultaneous production of hydrogen and oxygen gas at a current density of 10 mA/cm^2 and 100 mA/cm^2 at a cell voltage of 1.64 V and 1.98 V respectively. Owing to efficient HER and OER activities on Co—P—O, the geometric current of higher than 250 mA/cm^2 is produced in alkaline water. The electrocatalytic performance of Co—P—O nanoparticles deposited carbon cloth is compared with previous reports on state-of-the art catalyst electrode for alkaline electrolyser (Table 1), showing that overpotential for HER, OER and OWS are comparable or better than the electrodes based on cobalt phosphide. Even, the present electrolyser shows excellent stability towards electronic and mass transport for different current ranges from 10 to 100 mA/cm^2 (Fig. 5-b). The stability of Co—P—O catalysts was further measured for bi-functional catalysis by long-term chrono-potentiometry curve at 50 mA/cm^2 for 16 h (Fig. 5-c). The electrodes were investigated by powder XRD after the stability test as shown in Fig. 2-a and Fig. S6 respectively. The structure of the electrodes remains unchanged owing to the robust nature of the Co—P—O catalyst. The water dissociation step is extremely important in the alkaline condition. Previous DFT analysis suggest that the Co-sites in the oxygen doped cobalt phosphide adsorb water molecules more

effectively via capturing the O-atom through electrostatic interaction due to its more positive charge states as compared to pristine cobalt phosphide phase [41]. The effective adsorption of the water molecule of Co-sites leads to decreased water dissociation barrier, which enhances the HER rate in the alkaline condition. Rikai Liang et al report the Pt-like ΔG_{*H} for oxygen doped Co_2P, which leads to enhanced HER performance [41]. During oxygen evolution, OH– produced by water dissociation are effectively adsorbed on Co^{2+} sites and form CoO-OH_{ad}. The remaining OH– ions generates the other functional group and further oxidised to O2 molecule [41].

4. Conclusion

In summary, flexible, binder-free, and robust Co—P—O fabric has been fabricated by facile electroless plating and was used for water electrolysis. The remarkable HER and OER performance of Co—P—O is attributed to the presence of self-supported CoP and Co_3O_4 nanoparticles on CC, enabling a maximum current density of 400 mA/cm^2. During cathodic and anodic polarization, the close mechanical adherence and electrical connection of CC to Co—P—O facilitate the efficient transport of electrons, resulting in low charge transfer resistance. 3D design of Co—P—O ensures the presence of loose textures and open gaps among neighboring nano-porous Co—P—O nanoparticles. This arrangement facilitates the easy diffusion of the electrolyte into all the pores, thereby maximizing the utilization of Co-active sites. Utilizing Co—P—O electrodes, the two-electrode alkaline electrolysis system demonstrates effective water splitting at different current densities, achieving cell voltages of 1.64 V and 1.98 V for 10 and 100 mA/cm^2 and showing stability for time intervals of more than 16 h at 50 mA/cm^2 current density.

CRediT authorship contribution statement

Pooja J. Sharma: Writing – review & editing, Writing – original draft, Visualization, Validation, Software, Resources, Methodology, Investigation, Formal analysis, Data curation, Conceptualization. **Sohel Siraj:** Visualization, Resources, Formal analysis, Data curation. **Parikshit Sahatiya:** Visualization, Validation, Resources, Investigation, Formal analysis, Data curation. **C.K. Sumesh:** Visualization, Validation, Software, Resources, Investigation, Formal analysis. **Pratik M. Pataniya:** Writing – review & editing, Writing – original draft, Visualization, Validation, Supervision, Software, Resources, Project administration, Methodology, Investigation, Funding acquisition, Formal analysis, Data curation, Conceptualization.

Declaration of competing interest

The authors declare that they have no known competing financial interests or personal relationships that could have appeared to influence the work reported in this paper.

Acknowledgments

This work was financially supported by Charotar University of Science and Technology under CHARUSAT SEED GRANT FOR RESEARCH (CSGR)-PD3/22 (WATERSPLITTING). Ms. Pooja J. Sharma is thankful to CHARUSAT for Providing CPSF (CHARUSAT PhD Scholar Fellowship). The authors are thankful to CHARUSAT for providing research facilities.

Appendix A. Supplementary data

Supplementary data to this article can be found online at https://doi.org/10.1016/j.jelechem.2024.118491.

References

[1] S. Han, S. Liu, R. Wang, X. Liu, L. Bai, Z. He, One-step electrodeposition of nanocrystalline Zn x Co3–x O4 films with high activity and stability for electrocatalytic oxygen evolution, ACS Appl. Mater. Interfaces. 9 (2017) 17186–17194.
[2] C. Wang, H. Lu, Z. Mao, C. Yan, G. Shen, X. Wang, Bimetal Schottky heterojunction boosting energy-saving hydrogen production from alkaline water via urea electrocatalysis, Adv. Funct. Mater. 30 (2020) 2000556, https://doi.org/10.1002/adfm.202000556.
[3] L. Lei, Z. Yin, D. Huang, Y. Chen, S. Chen, M. Cheng, L. Du, Q. Liang, Metallic Co and crystalline Co-Mo oxides supported on graphite felt for bifunctional electrocatalytic hydrogen evolution and urea oxidation, J. Colloid Interface Sci. 612 (2022) 413–423, https://doi.org/10.1016/j.jcis.2021.12.149.
[4] X. Wang, J. Wang, X. Sun, S. Wei, L. Cui, W. Yang, J. Liu, Hierarchical coral-like NiMoS nanohybrids as highly efficient bifunctional electrocatalysts for overall urea electrolysis, Nano Res. 11 (2018) 988–996, https://doi.org/10.1007/s12274-017-1711-3.
[5] H. Wang, T. Liu, K. Bao, J. Cao, J. Feng, J. Qi, W doping dominated NiO / NiS 2 interfaced nanosheets for highly efficient overall water splitting, J. Colloid Interface Sci. 562 (2020) 363–369, https://doi.org/10.1016/j.jcis.2019.12.044.
[6] X. Liu, X. Wang, X. Yuan, W. Dong, F. Huang, Rational composition and structural design of in situ grown nickel-based electrocatalysts for efficient water electrolysis, J. Mater. Chem. A Mater. Energy Sustain. 4 (2015) 167–172, https://doi.org/10.1039/C5TA07047C.
[7] S. Gopi, A. Panda, A.G. Ramu, J. Theerthagiri, H. Kim, K. Yun, ScienceDirect Bifunctional electrocatalysts for water splitting from a bimetallic (V doped-NixFey) Metal e Organic framework MOF @ Graphene oxide composite, Int. J. Hydrogen Energy. (2021), https://doi.org/10.1016/j.ijhydene.2021.05.028.
[8] P. Zhou, X. Lv, D. Xing, F. Ma, Y. Liu, Z. Wang, P. Wang, Z. Zheng, Y. Dai, B. Huang, High-efficient electrocatalytic overall water splitting over vanadium doped hexagonal Ni0.2Mo0.8N, Appl. Catal. B Environ. 263 (2020) 118330, https://doi.org/10.1016/j.apcatb.2019.118330.
[9] S.Y. Liu, L. Wang, As featured, Sustain. Energy Fuels (2020), https://doi.org/10.1039/c9se00822e.
[10] L. Ma, K. Zhang, S. Wang, L. Gao, Y. Sun, Q. Liu, J. Guo, X. Zhang, Appl. Surf. Sci. (2019), https://doi.org/10.1016/j.apsusc.2019.06.044.
[11] Z. Cai, X. Bu, P. Wang, J.C. Ho, J. Yang, X. Wang, Recent advances in layered double hydroxide electrocatalysts for the oxygen evolution reaction, J. Mater. Chem. A 7 (2019) 5069–5089.
[12] P. Yu, F. Wang, T.A. Shifa, X. Zhan, X. Lou, F. Xia, J. He, Earth abundant materials beyond transition metal dichalcogenides: a focus on electrocatalyzing hydrogen evolution reaction, Nano Energy 58 (2019) 244–276.
[13] X. Du, J. Huang, J. Zhang, Y. Yan, C. Wu, Y. Hu, C. Yan, T. Lei, W. Chen, C. Fan, Modulating electronic structures of inorganic nanomaterials for efficient electrocatalytic water splitting, Angew. Chem. Int. Ed. 58 (2019) 4484–4502.
[14] A. Sahasrabudhe, H. Dixit, R. Majee, S. Bhattacharyya, Value added transformation of ubiquitous substrates into highly efficient and flexible electrodes for water splitting, Nat. Commun. 9 (2018) 2014, https://doi.org/10.1038/s41467-018-04358-7.
[15] P. Xu, Z. Bao, Y. Zhao, L. Zheng, Z. Lv, X. Shi, H. Wang, X. Fang, H. Zheng, Anionic regulation and heteroatom doping of ni-based electrocatalysts to boost biomass valorization coupled with hydrogen production, Adv. Energy Mater. 14 (2024) 2303557.
[16] L. Zheng, W. Ye, Y. Zhao, Z. Lv, X. Shi, Q. Wu, X. Fang, H. Zheng, Defect-induced atomic arrangement in CoFe bimetallic heterostructures with boosted oxygen evolution activity, Small. 19 (2023) 2205092.
[17] L. Zheng, W. Hu, X. Shu, H. Zheng, X. Fang, Ultrafine CoPx nanoparticles anchored on nitrogen doped reduced graphene oxides for superior hydrogenation in alkaline media, Adv. Mater. Interfaces. 5 (2018) 1800515.
[18] Y. Wang, B. Kong, D. Zhao, H. Wang, C. Selomulya, Strategies for developing transition metal phosphides as heterogeneous electrocatalysts for water splitting, Nano Today. 15 (2017) 26–55, https://doi.org/10.1016/j.nantod.2017.06.006.
[19] J. Tian, Q. Liu, A.M. Asiri, X. Sun, Self-supported nanoporous cobalt phosphide nanowire arrays: An, (2014) 14–17.
[20] G.-Q. Han, X. Li, Y.-R. Liu, B. Dong, W.-H. Hu, X. Shang, X. Zhao, Y.-M. Chai, Y.-Q. Liu, C.-G. Liu, Controllable synthesis of three dimensional electrodeposited Co–P nanosphere arrays as efficient electrocatalysts for overall water splitting, RSC Adv. 6 (2016) 52761–52771.
[21] J. Tian, Q. Liu, A.M. Asiri, X. Sun, Self-supported nanoporous cobalt phosphide nanowire arrays: an efficient 3D hydrogen-evolving cathode over the wide range of pH 0–14, J. Am. Chem. Soc. 136 (2014) 7587–7590.
[22] C.B. Sun, M.W. Guo, S.S. Siwal, Q.B. Zhang, Efficient hydrogen production via urea electrolysis with cobalt doped nickel hydroxide-riched hybrid films: cobalt doping effect and mechanism aspect, J. Catal. 381 (2020) 454–461, https://doi.org/10.1016/j.jcat.2019.11.034.
[23] J. Luo, J. Wang, Y. Guo, J. Zhu, H. Jin, Z. Zhang, D. Zhang, Y. Niu, S. Hou, J. Du, Metal-organic frameworks derived RuP2 with yolk-shell structure and efficient performance for hydrogen evolution reaction in both acidic and alkaline media, Appl. Catal. B Environ. 305 (2022) 121043.
[24] S. Huang, Z. Jin, P. Ning, C. Gao, Y. Wu, X. Liu, P. Xin, Z. Chen, Y. Jiang, Z. Hu, Synergistically modulating electronic structure of NiS2 hierarchical architectures by phosphorus doping and sulfur-vacancies defect engineering enables efficient electrocatalytic water splitting, Chem. Eng. J. 420 (2021) 127630.

[25] S. Chen, J. Duan, M. Jaroniec, S. Qiao, Nitrogen and oxygen dual-doped carbon hydrogel film as a substrate-free electrode for highly efficient oxygen evolution reaction, Adv. Mater. 26 (2014) 2925–2930.
[26] H. Jin, J. Wang, D. Su, Z. Wei, Z. Pang, Y. Wang, In situ cobalt–cobalt oxide/N-doped carbon hybrids as superior bifunctional electrocatalysts for hydrogen and oxygen evolution, J. Am. Chem. Soc. 137 (2015) 2688–2694.
[27] S.-H. Ye, J.-X. Feng, G.-R. Li, Pd nanoparticle/CoP nanosheet hybrids: highly electroactive and durable catalysts for ethanol electrooxidation, ACS Catal. 6 (2016) 7962–7969.
[28] B. Zhang, J. Liu, J. Wang, Y. Ruan, X. Ji, K. Xu, C. Chen, H. Wan, L. Miao, J. Jiang, Interface engineering: The Ni (OH) 2/MoS2 heterostructure for highly efficient alkaline hydrogen evolution, Nano Energy. 37 (2017) 74–80.
[29] P. Wang, B. Wang, CO-Co bond-stabilized CoP on carbon cloth toward hydrogen evolution reaction, Int. J. Hydrogen Energy 47 (2022) 9209–9219.
[30] L. Ji, J. Wang, X. Teng, T.J. Meyer, Z. Chen, CoP nanoframes as bifunctional electrocatalysts for efficient overall water splitting, ACS Catal. 10 (2020) 412–419, https://doi.org/10.1021/acscatal.9b03623.
[31] Y. Pan, K. Sun, S. Liu, X. Cao, K. Wu, W.-C. Cheong, Z. Chen, Y. Wang, Y. Li, Y. Liu, D. Wang, Q. Peng, C. Chen, Y. Li, Core-shell ZIF-8@ZIF-67-derived CoP nanoparticle-embedded N-doped carbon nanotube hollow polyhedron for efficient overall water splitting, J. Am. Chem. Soc. 140 (2018) 2610–2618, https://doi.org/10.1021/jacs.7b12420.
[32] P.M. Pataniya, V. Patel, P. Sahatiya, D.J. Late, C.K. Sumesh, Hydrogen evolution reaction in acidic and basic medium on robust cobalt sulphide electrocatalyst, Surf. Interfaces 34 (2022) 102319, https://doi.org/10.1016/j.surfin.2022.102319.
[33] S. Battiato, L. Bruno, A. Terrasi, S. Mirabella, Superior performances of electroless-deposited Ni-P films decorated with an ultralow content of Pt for water-splitting reactions, ACS Appl. Energy Mater. 5 (2022) 2391–2399, https://doi.org/10.1021/acsaem.1c03880.
[34] B.W. Zhang, S.Z. Liao, H.W. Xie, H. Zhang, Progress of electroless amorphous and nanoalloy deposition: a review–Part 1, Trans. IMF 91 (2013) 310–318.
[35] Y.-H. Lee, J.-S. Kim, J. Noh, I. Lee, H.J. Kim, S. Choi, J. Seo, S. Jeon, T.-S. Kim, J.-Y. Lee, Wearable textile battery rechargeable by solar energy, Nano Lett. 13 (2013) 5753–5761.
[36] M. Montazer, V. Allahyarzadeh, Electroless plating of silver nanoparticles/nanolayer on polyester fabric using AgNO3/NaOH and ammonia, Ind. Eng. Chem. Res. 52 (2013) 8436–8444.
[37] P.J. Sharma, K.H. Modi, P. Sahatiya, C.K. Sumesh, P.M. Pataniya, Electroless deposited NiP-fabric electrodes for efficient water and urea electrolysis for hydrogen production at industrial scale, Appl. Surf. Sci. 644 (2024) 158766, https://doi.org/10.1016/j.apsusc.2023.158766.
[38] S.M.S.I. Dulal, T.H. Kim, H. Rhee, J.Y. Sung, C.K. Kim, Development of an alkali-metal-free bath for electroless deposition of Co-W-P capping layers for copper interconnections, J. Alloys Compd. 467 (2009) 370–375, https://doi.org/10.1016/j.jallcom.2007.12.003.
[39] M. Schlesinger, Electroless deposition of nickel, Mod. Electroplat. Fifth Ed. 4 (2011) 447–458, https://doi.org/10.1002/9780470602638.ch18.
[40] Y. Yu, Z. Song, H. Ge, G. Wei, Preparation of CoP films by ultrasonic electroless deposition at low initial temperature, Prog. Nat. Sci. Mater. Int. 24 (2014) 232–238, https://doi.org/10.1016/j.pnsc.2014.04.004.
[41] R. Liang, J. Fan, F. Lei, P. Li, C. Fu, Z. Lu, W. Hao, Fabrication of ultra-stable and high-efficient CoP-based electrode toward seawater splitting at industrial-grade current density, J. Colloid Interface Sci. 645 (2023) 227–240, https://doi.org/10.1016/j.jcis.2023.04.143.
[42] Q. Guo, H. Shao, K. Zhang, G. Chen, W. Kong, X. Feng, Y. Gao, Y. Liu, N. Wang, C. Dong, F. Jiang, CoP nanoparticles intertwined with graphene nanosheets as a superior anode for half/full sodium-ion batteries, ChemElectroChem 8 (2021) 2022–2027, https://doi.org/10.1002/celc.202100085.
[43] K. Zhu, C. Jin, Z. Klencsár, A.S. Ganeshraja, J. Wang, Cobalt-iron oxide, alloy and nitride: synthesis, characterization and application in catalytic peroxymonosulfate activation for orange II degradation, Catalysts 7 (2017), https://doi.org/10.3390/catal7050138.
[44] F. Zhang, M. Wei, J. Sui, C. Jin, Y. Luo, S. Bie, R. Yang, Cobalt phosphide microsphere as an efficient bifunctional oxygen catalyst for Li-air batteries, J. Alloys Compd. 750 (2018) 655–658, https://doi.org/10.1016/j.jallcom.2018.04.070.
[45] Z. Xiao, Y. Wang, Y.-C. Huang, Z. Wei, C.-L. Dong, J. Ma, S. Shen, Y. Li, S. Wang, Filling the oxygen vacancies in Co 3 O 4 with phosphorus: an ultra-efficient electrocatalyst for overall water splitting, Energy Environ. Sci. 10 (2017) 2563–2569.
[46] P.M. Pataniya, X. Yang, B. Li, D. Kannichankandy, C.K. Sumesh, Enhanced electrocatalysis of WSe2 nanosheets by partial oxidation for hydrogen generation, Int. J. Energy Res. 46 (2022) 12073–12081, https://doi.org/10.1002/er.7971.
[47] N. Trivedi, M. Balal, V. Patel, S.R. Barman, C.K. Sumesh, P.M. Pataniya, Enhanced electrocatalytic performance of CuxNi1-xS Nanoflakes for overall water splitting, J. Electroanal. Chem. 944 (2023) 117648, https://doi.org/10.1016/j.jelechem.2023.117648.
[48] P.M. Pataniya, S. Dabhi, V. Patel, C.K. Sumesh, Liquid phase exfoliated ReS2 nanocrystals on paper based electrodes for hydrogen evolution and supercapacitor applications, Surf. Interfaces 34 (2022) 102318, https://doi.org/10.1016/j.surfin.2022.102318.
[49] L. Ma, X. Shen, H. Zhou, G. Zhu, Z. Ji, K. Chen, CoP nanoparticles deposited on reduced graphene oxide sheets as an active electrocatalyst for the hydrogen evolution reaction, J. Mater. Chem. A 3 (2015) 5337–5343.
[50] M.A.R. Anjum, M.S. Okyay, M. Kim, M.H. Lee, N. Park, J.S. Lee, Bifunctional sulfur-doped cobalt phosphide electrocatalyst outperforms all-noble-metal electrocatalysts in alkaline electrolyzer for overall water splitting, Nano Energy 53 (2018) 286–295, https://doi.org/10.1016/j.nanoen.2018.08.064.
[51] G. Chen, T. Wang, J. Zhang, P. Liu, H. Sun, X. Zhuang, M. Chen, X. Feng, Accelerated hydrogen evolution kinetics on NiFe-layered double hydroxide electrocatalysts by tailoring water dissociation active sites, Adv. Mater. 30 (2018) 1706279, https://doi.org/10.1002/adma.201706279.
[52] D. Wang, Q. Li, C. Han, Q. Lu, Z. Xing, X. Yang, Atomic and electronic modulation of self-supported nickel-vanadium layered double hydroxide to accelerate water splitting kinetics, Nat. Commun. 10 (2019) 3899, https://doi.org/10.1038/s41467-019-11765-x.
[53] R. Andaveh, A. Sabour Rouhaghdam, A. Seif, K. Wang, M. Maleki, J. Ai, G. Barati Darband, J. Li, In situ assembly of a superaerophobic CoMn/CuNiP heterostructure as a trifunctional electrocatalyst for ampere-level current density urea-assisted hydrogen production, ACS Appl. Mater. Interfaces (2024).
[54] S. Feng Zai, Y. Han Wu, Y. Tong Zhou, Z. Tian Hui Li, C. Bin Guo, Hierarchical NiOx nanotube arrays/CoP nanosheets heterostructure enables robust alkaline hydrogen evolution reaction, J. Colloid Interface Sci. 643 (2023) 350–359, https://doi.org/10.1016/j.jcis.2023.04.043.
[55] J. Tian, Q. Liu, A.M. Asiri, X. Sun, Self-supported nanoporous cobalt phosphide nanowire arrays, J. Am. Chem. Soc. 136 (2014) 7587–7590.
[56] A. Fathollahi, T. Shahrabi, G.B. Darband, Modulation of active surface sites on Ni–Fe–S by the dynamic hydrogen bubble template method for energy-saving hydrogen production, J. Mater. Chem. A 12 (2024) 9038–9054.
[57] H. Chen, B. Hui, Flexible NiFeP@ filter paper electrode for alkaline overall water electrosplitting, Int. J. Hydrogen Energy 51 (2024) 615–623.
[58] S. Battiato, L. Bruno, A.L. Pellegrino, A. Terrasi, S. Mirabella, Optimized electroless deposition of NiCoP electrocalysts for enhanced water splitting, Catal. Today 423 (2023) 113929.
[59] J.-G. Li, Y. Gu, H. Sun, L. Lv, Z. Li, X. Ao, X. Xue, G. Hong, C. Wang, Engineering the coupling interface of rhombic dodecahedral NiCoP/C@ FeOOH nanocages toward enhanced water oxidation, Nanoscale 11 (2019) 19959–19968.
[60] R. He, J. Li, L. Feng, NiCoP selenization for enhanced oxygen evolution reaction in alkaline electrolyte, Catal. Commun. 163 (2022) 106407.
[61] H. Huang, C. Yu, J. Yang, C. Zhao, X. Han, Z. Liu, J. Qiu, Strongly coupled architectures of cobalt phosphide nanoparticles assembled on graphene as bifunctional electrocatalysts for water splitting, ChemElectroChem 3 (2016) 719–725.
[62] P. Wang, F. Song, R. Amal, Y.H. Ng, X. Hu, Efficient water splitting catalyzed by cobalt phosphide-based nanoneedle arrays supported on carbon cloth, ChemSusChem 9 (2016) 472–477.
[63] Y. Zhu, Y. Liu, T. Ren, Z. Yuan, Self-supported cobalt phosphide mesoporous nanorod arrays: a flexible and bifunctional electrode for highly active electrocatalytic water reduction and oxidation, Adv. Funct. Mater. 25 (2015) 7337–7347.
[64] Y. Bai, H. Zhang, Y. Feng, L. Fang, Y. Wang, Sandwich-like CoP/C nanocomposites as efficient and stable oxygen evolution catalysts, J. Mater. Chem. A 4 (2016) 9072–9079.
[65] J. Wang, W. Yang, J. Liu, CoP 2 nanoparticles on reduced graphene oxide sheets as a super-efficient bifunctional electrocatalyst for full water splitting, J. Mater. Chem. A 4 (2016) 4686–4690.
[66] L. Jiao, Y.-X. Zhou, H.-L. Jiang, Metal–organic framework-based CoP/reduced graphene oxide: high-performance bifunctional electrocatalyst for overall water splitting, Chem. Sci. 7 (2016) 1690–1695.
[67] B. Qiu, L. Cai, Y. Wang, Z. Lin, Y. Zuo, M. Wang, Y. Chai, Fabrication of nickel–cobalt bimetal phosphide nanocages for enhanced oxygen evolution catalysis, Adv. Funct. Mater. 28 (2018) 1706008.
[68] W. Jin, J. Chen, H. Wu, N. Zang, Q. Li, W. Cai, Z. Wu, Interface engineering of oxygen-vacancy-rich NiCo 2 O 4/NiCoP heterostructure as an efficient bifunctional electrocatalyst for overall water splitting, Catal. Sci. Technol. 10 (2020) 5559–5565.